Syntaxin 11 regulates the stimulus-dependent transport of Toll-like receptor 4 to the plasma membrane by cooperating with SNAP-23 in macrophages

Daiki Kinoshita, Chiye Sakurai, Maya Morita, Masashi Tsunematsu, Naohiro Hori, and Kiyotaka Hatsuzawa*
Division of Molecular Biology, School of Life Sciences, Faculty of Medicine, Tottori University, Yonago, Tottori 683-8503, Japan

ABSTRACT Syntaxin 11 (stx11) is a soluble *N*-ethylmaleimide–sensitive factor attachment protein receptor (SNARE) that is selectively expressed in immune cells; however, its precise role in macrophages is unclear. We showed that *stx11* knockdown reduces the phagocytosis of *Escherichia coli* in interferon-γ–activated macrophages. *stx11* knockdown decreased Toll-like receptor 4 (TLR4) localization on the plasma membrane without affecting total expression. Plasma membrane–localized TLR4 was primarily endocytosed within 1 h by lipopolysaccharide (LPS) stimulation and gradually relocalized 4 h after removal of LPS. This relocalization was significantly impaired by *stx11* knockdown. The lack of TLR4 transport to the plasma membrane is presumably related to TLR4 degradation in acidic endosomal organelles. Additionally, an immunoprecipitation experiment suggested that stx11 interacts with SNAP-23, a plasma membrane–localized SNARE protein, whose depletion also inhibits TLR4 replenishment in LPS-stimulated cells. Using an intramolecular Förster resonance energy transfer (FRET) probe for SNAP-23, we showed that the high FRET efficiency caused by LPS stimulation is reduced by *stx11* knockdown. These findings suggest that stx11 regulates the stimulus-dependent transport of TLR4 to the plasma membrane by cooperating with SNAP-23 in macrophages. Our results clarify the regulatory mechanisms underlying intracellular transport of TLR4 and have implications for microbial pathogenesis and immune responses.

INTRODUCTION

Toll-like receptors (TLRs) play critical roles in the recognition of microbial components and the induction of innate and adaptive immunity (Takeuchi and Akira, 2010). Lipopolysaccharide (LPS), a highly immunostimulatory outer membrane component of Gram-negative bacteria, is detected by TLR4, which induces several inflammatory responses and endotoxic shock (Bryant *et al.*, 2010). The stimulation of TLR4 by LPS at the plasma membrane promotes recruitment of the adaptor protein myeloid differentiation factor 88, leading to activation of the transcription factor nuclear factor κB and expression of proinflammatory cytokines (Akira and Takeda, 2004). TLR4-bound LPS is then internalized into endocytic organelles by regulatory factors, such as CD14 (Zanoni *et al.*, 2011), resulting in recruitment of the adaptor proteins Toll-interleukin-1 receptor domain–containing adaptor inducing interferon-β and Toll-receptor–associated molecule. This activates the transcription factor interferon regulatory factor-3, which regulates type I interferon (IFN)

expression (Kagan *et al.*, 2008). These distinct localization-dependent signaling pathways indicate that regulation of the intracellular transport of TLR4 is a profoundly important process.

The newly translated TLR4 in the endoplasmic reticulum (ER) is regulated by two ER-resident chaperone molecules, glycoprotein 96 and protein associated with TLR4, for proper transport to the plasma membrane (Randow and Seed, 2001; Wakabayashi *et al.*, 2006; Takahashi *et al.*, 2007). The TLR4 receptor complex—composed of TLR4 and myeloid differentiation factor 2 (MD2)—in the ER also interacts with transmembrane emp24 domain–containing protein 7 (TMED7), which belongs to the TMED/p24-family of cargo receptors, during anterograde ER-to-Golgi transport (Liaunardy-Jopeace *et al.*, 2014). Moreover, the small GTPase Rab10 is required for transport of the fully glycosylated TLR4 receptor complex from the Golgi to the plasma membrane, which occurs in both constitutive and LPS-regulated secretory pathways (Wang *et al.*, 2010). Depending on cell type, TLR4 is localized not only on the plasma membrane but also in the Golgi, endocytic recycling compartment (ERC), and endomembrane structures (Liaunardy-Jopeace and Gay, 2014). However, the membrane fusion molecules responsible for the transport of TLR4 from its intracellular organelles to the plasma membrane have not been identified.

During the intracellular trafficking of cargo proteins, soluble *N*-ethylmaleimide–sensitive factor attachment protein receptor (SNARE) proteins, which are the most common fusogenic factors on the two membranes, form complexes with each other to promote membrane fusion. These complexes contain coiled-coil bundles consisting of four helices; the Qa-, Qb-, and Qc-SNARE motifs are from SNAREs of the syntaxin and SNAP-25 families, while the R-SNARE motif is from the vesicle-associated membrane protein (VAMP, also called synaptobrevin) SNARE family (Fasshauer *et al.*, 1998; Jahn and Scheller, 2006; Hong and Lev, 2014). Syntaxin 11 (stx11) is an atypical member of the Q-SNARE family that lacks the transmembrane domain and is selectively expressed in various tissues and cells of the immune system (Prekeris *et al.*, 2000; Bryceson *et al.*, 2007; Offenhäuser *et al.*, 2011). While stx11 associates with membranes by palmitoylation of cysteine residues at its C-terminus, stx11-mediated membrane fusion can be entirely achieved by the chaperone function of the Sec/Munc protein Mun18-2 (Zhou *et al.*, 2013; Hellewell *et al.*, 2014; Spessott *et al.*, 2017). Furthermore, stx11 expression increases in response to LPS or IFN-γ in macrophages and dendritic cells (Zhang *et al.*, 2008; D'Orlando *et al.*, 2013; Collins *et al.*, 2015; Naegelen *et al.*, 2015).

In cytotoxic T-lymphocytes (CTLs) and natural killer (NK) cells, upon recognition of virally infected or tumor target cells, stx11 is involved in the fusion of lytic granules with the plasma membrane during exocytosis toward the contact site, called the immunological synapse, between the two cells (de Saint Basile *et al.*, 2010; D'Orlando *et al.*, 2013; Chang *et al.*, 2017). Exocytosis of platelet granules also requires stx11 (Ye *et al.*, 2012). In primary human monocytes and macrophages, *stx11* knockdown enhances the phagocytotic efficiency of apoptotic cells and immunoglobulin G (IgG)-opsonized red blood cells (Zhang *et al.*, 2008). In contrast, stx11 deficiency does not affect phagocytosis in macrophages (D'Orlando *et al.*, 2013). Furthermore, it has been reported that stx11 regulates intracellular trafficking steps between late endosomes, lysosomes, and the plasma membrane, rather than phagocytosis in macrophages (Offenhäuser *et al.*, 2011). Thus, it is unclear whether stx11 functions in membrane trafficking in macrophages and which SNARE proteins interact with stx11 in the process.

In the present study, we found that stx11 in macrophages is predominately localized on the plasma membrane and that *stx11* knockdown results in remarkable inhibition of TLR4 transport to the cell surface in response to activation by IFN-γ or LPS. Similar inhibitory effects were also observed in cells with suppressed expression of SNAP-23 (synaptosomal-associated protein 23 kDa; a plasma membrane—localized Qbc-SNARE), which interacts with stx11. The structural alteration of SNAP-23 caused by LPS activation was undetectable in *stx11*-knockdown cells. Thus, our data suggest that stx11 regulates the stimulus-dependent transport of TLR4 to the plasma membrane by cooperating with SNAP-23 in macrophages.

RESULTS

Knockdown of *stx11* inhibits the phagocytosis of *Escherichia coli* in IFN-γ–activated macrophages

To investigate the role of stx11 in macrophage intracellular membrane trafficking, we designed small interfering RNAs (siRNAs) targeting the noncoding region (siRNA#1) and coding region (siRNA#2) of mouse *stx11* mRNA. After transfection of these siRNAs into J774 cells (a murine macrophage-like line), siRNA#1 was found to reduce stx11 expression more effectively than did siRNA#2 (Figure 1A). As shown in Figure 1B, this reduction was observed in IFN-γ–activated J774 cells without affecting the IFN-γ–induced expression of LRG47 (MacMicking, 2004), whereas IFN-γ enhanced stx11 expression in control siRNA-transfected cells (Zhang *et al.*, 2008; D'Orlando *et al.*, 2013). This effect was confirmed by immunofluorescence using anti-stx11 antibodies, which indicated that stx11 is mainly localized on the plasma membrane (Figure 1C).

We then examined the effects of stx11 siRNA#1 on Fc receptor (FcR)-mediated phagocytosis by measuring the uptake of Texas Red–conjugated zymosan particles opsonized with IgG. Phagocytotic efficiency did not differ between J774 cells transfected with stx11 siRNA#1 and control cells, although the efficiency was significantly enhanced by IFN-γ in both cells (Figure 1D). Next, we investigated the effect of *stx11* knockdown on the phagocytosis of *Escherichia coli* particles expressing the glutathione *S*-transferase–tagged mCherry-mVenus tandem protein, in which phagocytotic efficiency is indicated by the mCherry fluorescence intensity, and phagosome maturation (acidification) is indicated by the mVenus:mCherry fluorescence intensity ratio (Morita *et al.*, 2017). At the steady state, phagocytotic efficiency of the particles did not differ between *stx11*-knockdown cells and control cells (Figure 1E). However, phagocytotic efficiency increased in control siRNA-transfected cells via IFN-γ activation. This increase was not observed in *stx11*-knockdown cells (Figure 1E). To clarify whether *stx11* knockdown affects phagosome formation or the association between particles and the cell surface, we examined association efficiency of the *E. coli*-mCherry-mVenus particles. As shown in Figure 1F, a significant increase in association efficiency in response to IFN-γ activation in control cells was not observed in *stx11*-knockdown cells. These results suggest that stx11 is involved in the phagocytosis of *E. coli* particles, especially in IFN-γ–activated macrophages.

Knockdown of *stx11* inhibits the surface expression of TLR4 in IFN-γ–activated macrophages

Escherichia coli particles are recognized by surface-expressed receptors such as TLR4, whose specific ligand is LPS. Thus, the effect of *stx11* knockdown on the surface expression of TLR4 was examined by immunofluorescence. TLR4 expression was significantly enhanced in control cells upon IFN-γ activation, but the same was not observed in *stx11*-knockdown cells (Figure 2, A and B).
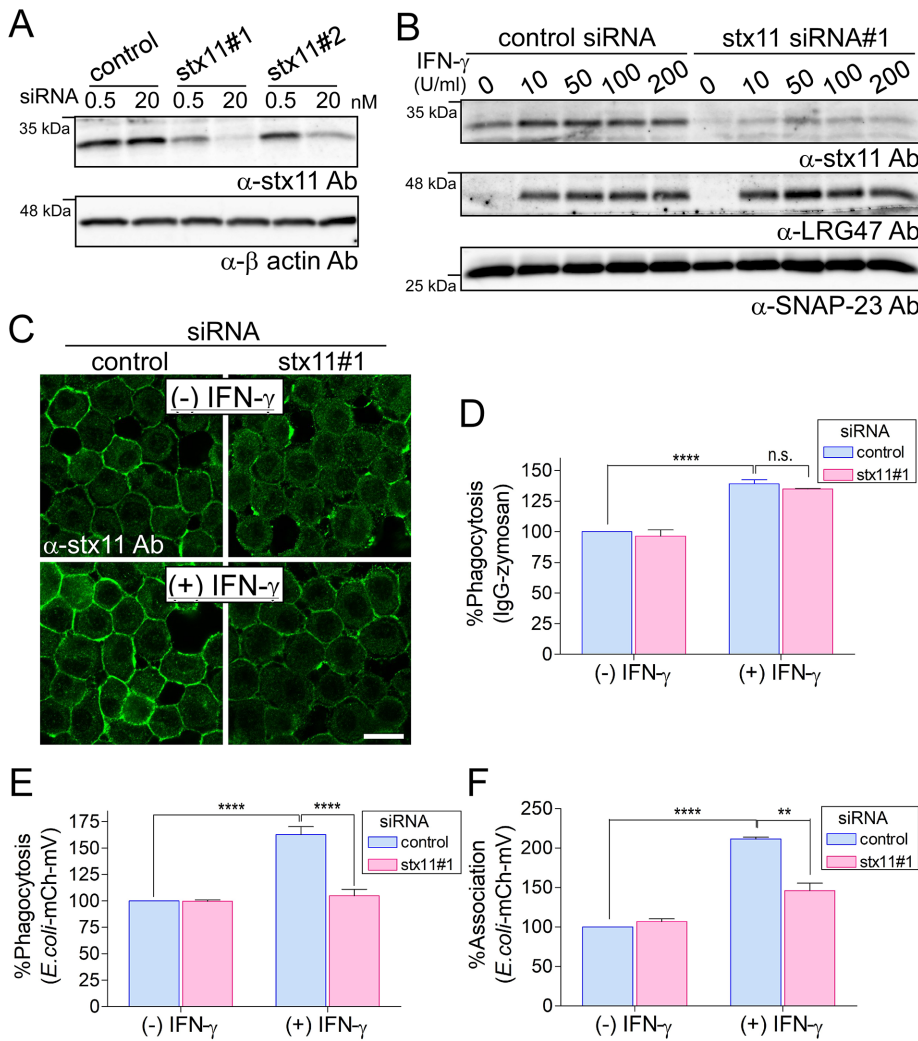
FIGURE 1: Knockdown of *stx11* inhibits the phagocytosis of *E. coli* in IFN-γ–activated macrophages. (A) J774 cells were transfected with stx11 siRNAs (#1 and #2) or a nonspecific siRNA control. Total lysates from siRNA-transfected cells were analyzed by Western blotting using the indicated antibodies. (B) J774 cells transfected with siRNAs were incubated in the presence of IFN-γ at the indicated concentrations for 12 h. Total-cell lysates were analyzed by Western blotting using the indicated antibodies. LRG47 is an IFN-γ–inducible GTPase used as a positive marker for IFN-γ signals. (C) J774 cells transfected with siRNAs were incubated in the presence or absence of IFN-γ (100 U/ml) for 12 h. Cells were then fixed and stained with anti-stx11 antibodies. The plasmalemmal staining of stx11 was efficiently reduced in the absence of IFN-γ and was down-regulated even in IFN-γ–activated cells. Scale bar: 10 μm. (D–F) siRNA-transfected J774 cells were incubated in the presence or absence of IFN-γ (100 U/ml) for 12 h. Cells were further incubated with IgG-opsonized Texas Red-zymosan or *E. coli*-mCherry-mVenus particles, and then the efficiencies (%) of (D, E) phagocytosis and (F) associations were measured as described in *Materials and Methods*. Fluorescence values for each cell line were normalized to the maximal value obtained from control siRNA-transfected cells within the same experiment, which was arbitrarily defined as 100%. Data are presented as the means ± SE of three independent experiments. Statistical analyses were performed using one-way ANOVA with Tukey's post hoc tests (**, $p < 0.01$; ****, $p < 0.001$).

Because immunofluorescence analysis was performed using cells without detergent permeabilization, it is not clear whether intracellular TLR4 accumulates or is degraded in *stx11*-knockdown cells treated with IFN-γ. Therefore, lysates from cells in each condition were subjected to Western blot analysis to quantify total TLR4; *stx11* knockdown appeared to not affect the stability of TLR4 within cells (Figure 2C). For another surface receptor, CD64 (FcγRIa), expression was enhanced on the plasma membrane of IFN-γ–activated J774 cells but was not altered after transfection with stx11 siRNA#1 (Figure 2, D and E). These results suggest that stx11 selectively regulates TLR4 transport to the plasma membrane in macrophages depending on IFN-γ activation.

Knockdown of *stx11* inhibits the replenishment of TLR4 on the plasma membrane in LPS-stimulated macrophages

Although TLR4 is required to induce inflammatory endocytosis in response to its ligand LPS and is replenished on the plasma membrane before the next round of stimulation (Zanoni *et al.*, 2011), the molecular mechanism underlying intracellular TLR4 trafficking is not fully understood. For investigation of the effect of LPS stimulation on the localization of TLR4, J774 cells were transfected with siRNAs and incubated for several hours in the presence of LPS. As shown in Supplemental Figure S1, A and B, the fluorescence signal of surface TLR4 was reduced by more than half in both control and stx11 siRNA#1–transfected cells within 1 h of incubation. TLR4 surface expression recovered to almost steady-state levels over time in control cells but not in *stx11*-knockdown cells. These results can be partially attributed to TLR4 that is transported to and endocytosed from the plasma membrane. To purely observe TLR4 transport to the plasma membrane, we stimulated J774 cells with LPS for 1 h, removed LPS, and incubated the cells without LPS for an additional 2 and/or 4 h. Around 1.5-fold more TLR4 than originally present became localized to the plasma membrane up to 4 h after incubation without LPS (Figure 3, A and B). As shown in Supplemental Figure S1, A and B, cells transfected with stx11 siRNA#1 showed a remarkable reduction in TLR4 replenishment compared with that of control cells, without effecting endocytosis (Figure 3, A and B). However, the total amount of TLR4 at each time point did not change substantially in either cell type (Supplemental Figures S1C and S2). To determine the specificity of knockdown effects with stx11 siRNA#1, we performed a rescue experiment in which the siRNA-transfected cells were transiently transfected with mVenus-tagged protein overnight, treated with LPS for 1 h, and then incubated without LPS for 4 h. After the cells were immunostained with anti-TLR4 antibodies, the number of cells with strongly replenished TLR4 on the plasma membrane among cells expressing mVenus-tagged proteins was quantitated by microscopy. As shown in Figure 3, C and D, the overexpression of mVenus-stx11 notably
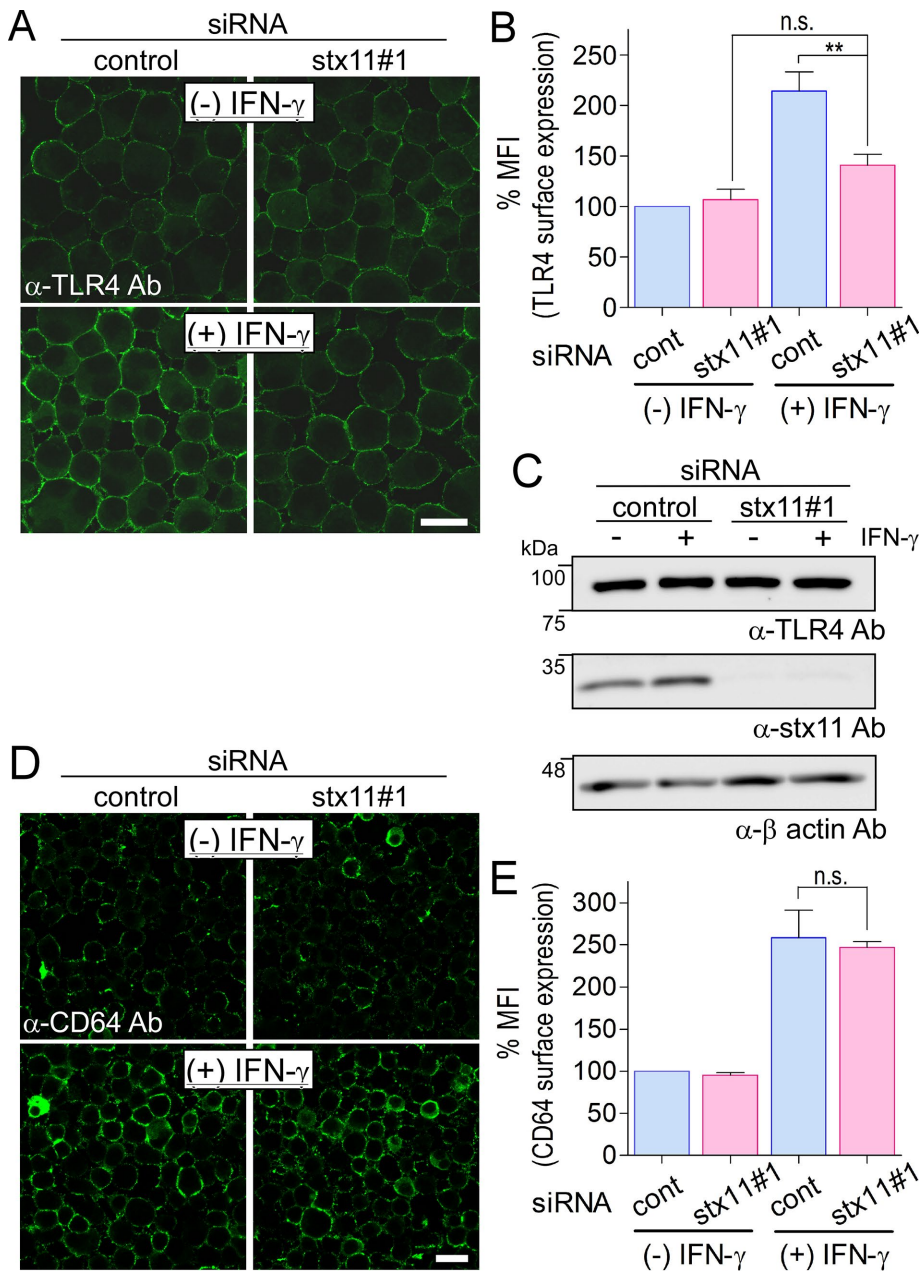
FIGURE 2: Knockdown of *stx11* inhibits the surface expression of TLR4 in IFN-γ–activated macrophages. (A) J774 cells transfected with siRNAs (control or stx11 siRNA#1) were incubated in the presence or absence of IFN-γ (100 U/ml) for 12 h. Cells were directly stained with anti-TLR4 antibodies followed by fluorescent dye–conjugated goat anti-mouse secondary antibodies without permeabilization of the plasma membrane before fixation. (B) Fluorescence intensity of the plasma membrane of each cell (of at least 30 cells) from A was quantified using ImageJ. Each intensity value was normalized to the intensity of control cells in the absence of IFN-γ, defined as 100%. Data are presented as the means ± SE of five independent experiments. Statistical analysis was performed using one-way ANOVA with Tukey's post hoc tests (**, $p <$ 0.01). (C) Total lysates from siRNA-transfected cells in A were analyzed by Western blotting using the indicated antibodies. (D) As a control, cells were also directly stained with anti-CD64 antibodies as described in A. (E) Fluorescence intensity of the plasma membrane of each cell from D was quantified and analyzed as described in B. Data are presented as the means ± SE of three independent experiments. Scale bar: 10 μm.

Endocytosed TLR4 was recycled to the plasma membrane for replenishment, but was transported to lysosomes in *stx11*-knockdown cells

Around half of the cell surface–localized TLR4 was endocytosed within 1 h in LPS-stimulated macrophages, whereas more than the original amount of surface TLR4 was replenished on the plasma membrane after LPS removal. To investigate replenishment of intracellular TLR4 in response to LPS, we examined the inhibition of de novo protein synthesis using puromycin or inhibition of transport between the ER and Golgi by BFA. J774 cells were stimulated with LPS for 1 h and then incubated for an additional 4 h without LPS in the presence or absence of either reagent. TLR4 levels of cells treated with puromycin or BFA were replenished to the same level as before stimulation but did not surpass that of the vehicle (Figure 4, A and B). This recovery of TLR4 appeared to originate from endocytosed TLR4 via the endosomal recycling pathway. It was confirmed that puromycin and BFA inhibited de novo TLR4 synthesis and caused dispersion of TLR4 throughout the cytoplasm into small dot-like structures, respectively, in permeabilized macrophages that were treated under the same conditions as in Figure 4A (Supplemental Figure S3). These results suggest that total replenishment of TLR4 comes from at least both the recycling and de novo synthesis pathways and that stx11 may regulate membrane fusion of vesicles (or compartments) from the ERC with the plasma membrane. Next, to investigate localization of intracellular TLR4 in *stx11*-knockdown cells, immunofluorescence assays were performed accompanied with permeabilization. Cells were stimulated with LPS for 1 h and then incubated without LPS for 4 h before being immunostained. No remarkable difference in staining with anti-TLR4 antibodies was observed between control and *stx11*-knockdown cells (Figure 4C). This result indicates that TLR4 that is not transported to the plasma membrane in *stx11*-knockdown cells may be mislocalized to lysosomes for degradation. The LPS stimulation experiment was reexamined in the presence of a protease inhibitor cocktail to clarify this. As shown in Figure 4C, immunofluorescence intensity of anti-TLR4 antibodies was markedly increased in lysosomal associated membrane pro-

restored the surface expression of TLR4 compared with that of mVenus, indicating that stx11 plays an essential role in intracellular TLR4 transport to the plasma membrane in LPS-stimulated macrophages.

tein 1 (LAMP-1)-positive compartments in *stx11*-knockdown cells. These results suggest that a population of TLR4 not replenished on the plasma membrane due to stx11 depletion is transported to lysosomes.
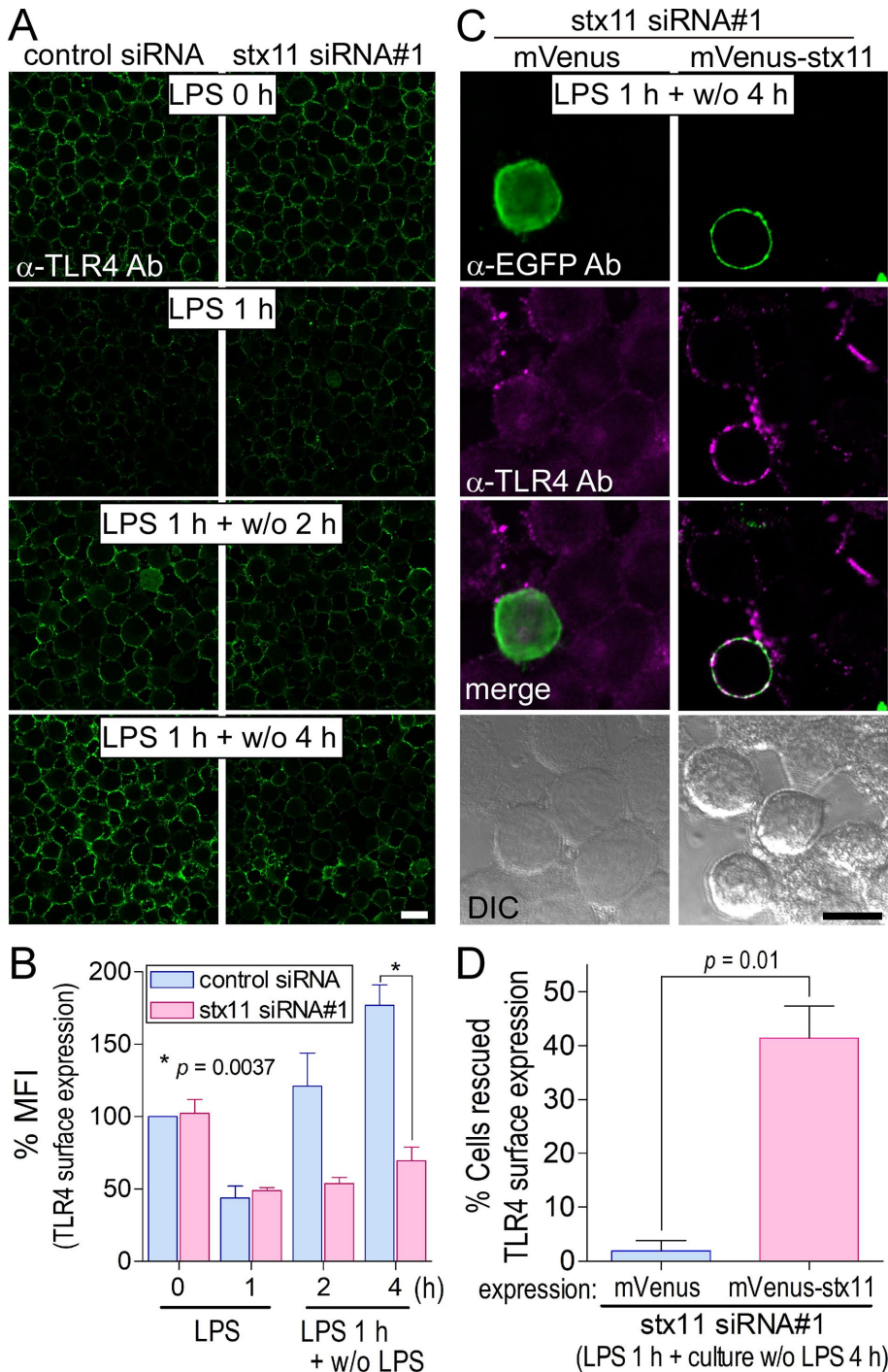
FIGURE 3: Knockdown of *stx11* inhibits the replenishment of TLR4 on the plasma membrane in LPS-stimulated macrophages. (A) At 72 h after transfection with siRNAs (control or stx11 siRNA#1), cells were treated with LPS (1 μg/ml) for 1 h (LPS 1 h). After LPS was washed out, the cells were further incubated without LPS for the indicated times (LPS 1 h + w/o 2 h or LPS 1 h + w/o 4 h). Cells were directly stained with anti-TLR4 antibodies as described in Figure 2A. (B) Fluorescence intensity of the plasma membrane of each cell (of at least 30 cells) from A was quantified using ImageJ. Each intensity value was normalized to that of control cells in the absence of LPS, defined as 100%. Data are presented as the means ± SE of three independent experiments. (C) At 54 h after the transfection of stx11 siRNA#1, cells were transfected with plasmids expressing mVenus or mVenus-stx11 and incubated for 18 h. After stimulation with LPS (1 μg/ml) for 1 h, the cells were incubated for another 4 h without LPS. TLR4 surface expression was visualized as described in A, and the cells were permeabilized and stained with anti-EGFP antibodies followed by fluorescent dye–conjugated goat anti-rabbit secondary antibodies. TLR4 surface expression was partially rescued by the expression of mVenus-stx11 but not mVenus.

TLR4-mVenus is replenished via the ERC on the plasma membrane upon LPS stimulation

stx11 was mainly localized on the plasma membrane in macrophages (Figure 1C), indicating that it may regulate the membrane fusion of intracellular compartment(s) with the plasma membrane to replenish TLR4. In *stx11*-knockdown cells, intracellular TLR4 from both endocytosis and de novo synthesis pathways dependent on LPS stimulation was transported to lysosomes (Figure 4C). To answer the question of where this TLR4 population is transported to lysosomes, *stx11*-knockdown cells in the presence of bafilomycin A1 (BafA1; 10 nM), a specific inhibitor of vacuolar-type H⁺-ATPase, were stimulated with LPS for 1 h and incubated without LPS for an additional 4 h. The cells were immunostained with antibodies against TLR4 and LAMP-1 under permeabilized conditions. As shown in Supplemental Figure S4, treatment with BafA1 caused TLR4 accumulation in a large dot-like structure, but we have no appropriate antibodies against several marker proteins to detect this structure. Therefore, we established a J774 cell line overexpressing both mVenus-tagged TLR4 (TLR4-mV) and its FLAG-tagged cofactor MD2 (MD2-Flag) to visualize TLR4 trafficking. Expressed TLR4-mV was localized on the plasma membrane and partially in the intracellular compartments (Supplemental Figure S5 and Figure 5A). Consistent with endogenous TLR4, the amount of plasma membrane–localized TLR4-mV decreased 1 h after LPS stimulation and was subsequently recovered after incubation without LPS for 4 h (control siRNA; Figure 5, A and B). When J774/TLR4-mV and MD2-Flag cells were transfected with stx11 siRNA#1, the replenishment of TLR4-mV on the plasma membrane was significantly suppressed compared with that of the control (Figure 5, A and B), indicating that stx11 regulates TLR4-mV transport to the plasma membrane as well as endogenous TLR4 in LPS-stimulated macrophages. The remarkable intracellular accumulation of TLR4-mV was also not detected even 4 h

(D) The number of cells apparently expressing TLR4 on the plasma membrane was analyzed by microscopy. Results are expressed as the percentage of TLR4-stained cells in cells expressing the mVenus-tagged protein (10–16 cells for each experiment). Data are presented as the means ± SE of four independent experiments. Statistical analysis was performed using two-tailed, paired Student's *t* tests. Scale bar: 10 μm.
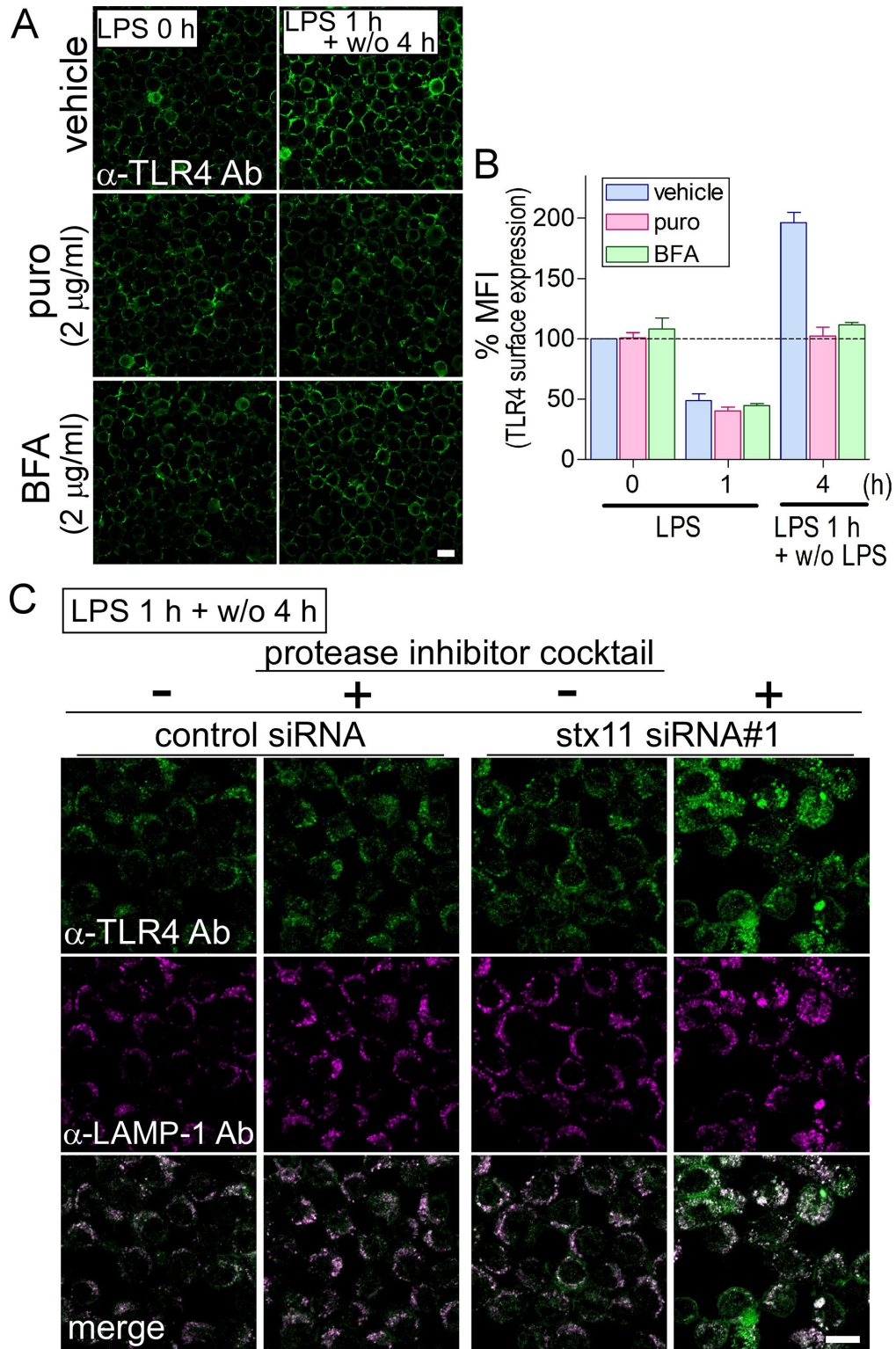
FIGURE 4: Endocytosed TLR4 is recycled back to the plasma membrane for replenishment, but is transported to lysosomes in *stx11*-knockdown cells. (A) In the presence or absence of puromycin (puro: 2 µg/ml) or brefeldin A (BFA: 2 µg/ml), J774 cells (LPS 0 h) were treated with LPS (1 µg/ml) for 1 h and then further incubated without LPS for 4 h after LPS was washed out (LPS 1 h + w/o 4 h). Cells were directly stained with anti-TLR4 antibodies, and then the fluorescence intensity of plasma membranes was quantified as described in Figure 2A. (B) Fluorescence intensity of the plasma membrane of each cell (of at least 30 cells) from A was quantified and analyzed as described in Figure 2B. Data are presented as the means ± SE of three independent experiments. (C) At 72 h after transfection with siRNAs (control or stx11 siRNA#1), cells were treated with LPS as described in A in the presence or absence of a protease inhibitor cocktail (Nacalai Tesque; LPS 1 h + w/o 4 h). Under permeabilized conditions, cells were stained with antibodies against TLR4 and LAMP-1 followed by fluorescent dye–conjugated goat anti-mouse and rat secondary antibodies, respectively. Scale bar: 10 µm.
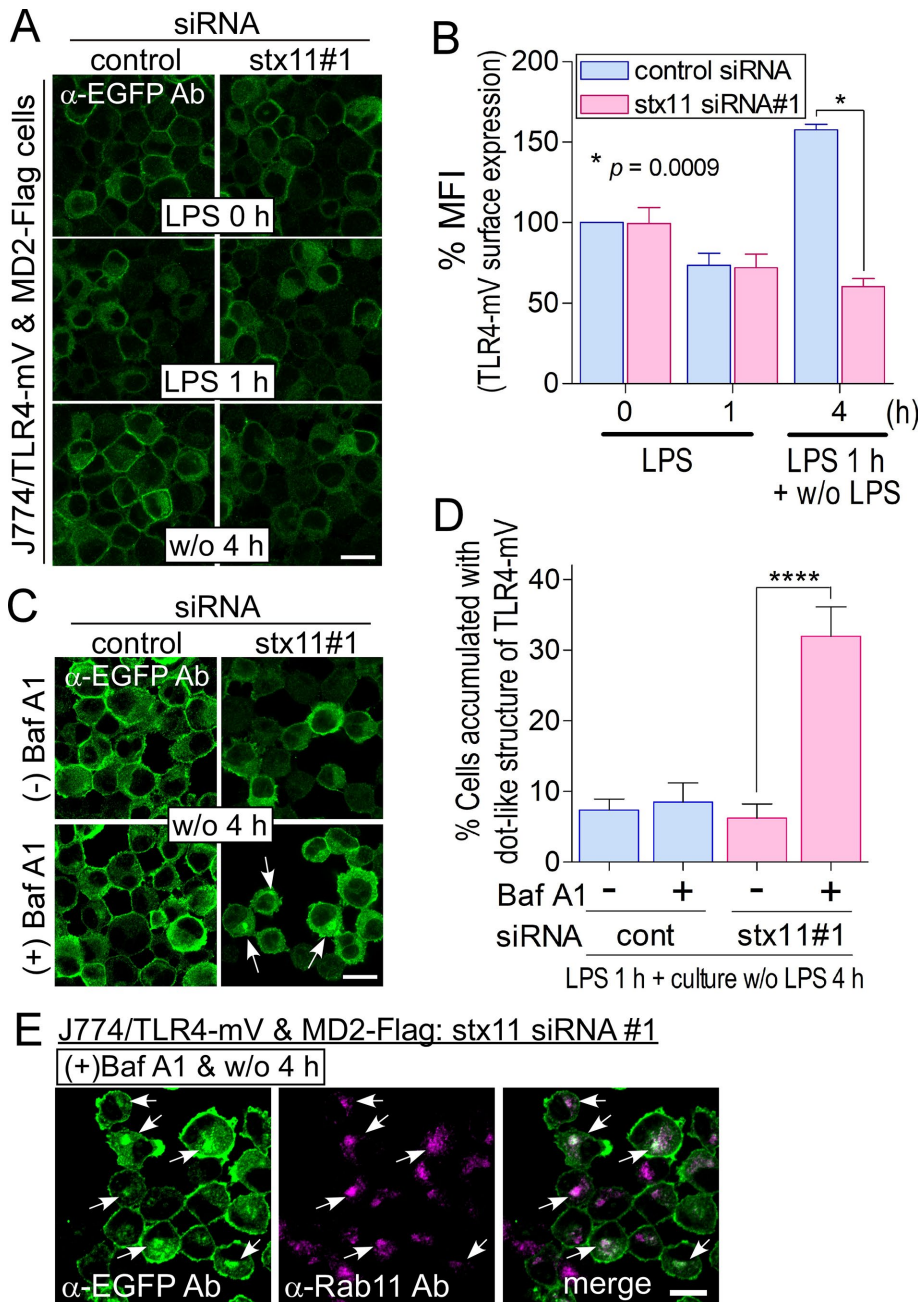
FIGURE 5: TLR4-mVenus is replenished via BafA1-sensitive compartments upon LPS stimulation. (A) J774 cells expressing TLR4-mVenus and MD2-Flag (J774/TLR4-mV and MD2-Flag cells) were treated with siRNAs and LPS as described in Figure 3A. The cells were stained with anti-EGFP antibodies followed by fluorescent dye–conjugated goat anti-rabbit secondary antibodies. (B) Fluorescence intensity of the plasma membrane of each cell (of at least 30 cells) from A was quantified using ImageJ. Each intensity value was normalized to that of control cells in the absence of LPS, defined as 100%. Data are presented as the means ± SE of three independent experiments. (C) siRNA-transfected J774/TLR4-mV and MD2-Flag cells were treated with LPS for 1 h and then incubated for an additional 4 h without LPS in the presence or absence of BafA1 (final: 10 nM). Imaging analysis was performed as described in A. (D) The number of accumulated cells of distinct dot-like structures of TLR4-mV was analyzed by microscopy. Results are expressed as the percentage of cells accumulating dot-like structures of TLR4-mV (more than 35 cells for each experiment). Data are presented as the means ± SE of four independent experiments. (E) J774/TLR4-mV and MD2-Flag cells were treated as described in C. The cells were fixed and stained with anti-EGFP and anti-Rab11 antibodies followed by fluorescent dye–conjugated secondary antibodies. Statistical analyses were performed using two-tailed, paired Student's *t* tests (B) or one-way ANOVA with Tukey's post hoc tests (D; ****, *p* < 0.001). White arrows indicate accumulated dot-like structures of TLR4-mV. Scale bar: 10 μm.

after LPS removal in *stx11*-knockdown cells (Figure 5A). Although no difference in total TLR4-mV in the cells stimulated with or without LPS was observed via Western blotting (Supplemental Figure S5C), endocytosed TLR4-mV may be transported to lysosomes for degradation in *stx11*-knockdown cells. Treatment with BafA1 did not affect TLR4-mV endocytosis 1 h after LPS stimulation in control and stx11 siRNA#1 cells or the subsequent replenishment of TLR4-mV on the plasma membrane in control cells (unpublished data). In contrast, TLR4-mV, as well as endogenous TLR4, accumulated in the large dot-like structure in around 30% of *stx11*-knockdown cells in the presence of BafA1 after stimulation and subsequent incubation for 4 h without LPS (Figure 5, C and D). This structure was close to the *cis*-Golgi marker GM130 and slightly overlapped with the late endosome/lysosome marker LAMP-1 and the early endosome marker EEA1; furthermore, the ERC marker Rab11 exhibited considerable colocalization with the accumulated TLR4-mV structure (Supplemental Figure S6 and Figure 5E). Considering that BafA1 neutralizes acidic endosomes/lysosomes and inhibits intracellular transport between these organelles (Okiyoneda *et al.*, 2006)—especially from the endosomes to lysosomes (Baravalle *et al.*, 2005)—these results suggest that TLR4-mV, which is included in carrier vesicle(s) from the ERC in *stx11*-knockdown cells stimulated with LPS, may be transported to lysosomes for degradation. Therefore, TLR4-mV may be replenished via the Rab11-positive ERC upon LPS stimulation.

SNAP-23 mediates LPS-induced TLR4 transport to the plasma membrane in macrophages as well as constitutive transport

To further analyze the function of stx11, we established J774 cells overexpressing mVenus-tagged stx11 (mV-stx11). As shown in Figure 6A, overexpressed mV-stx11 was mostly localized on the plasma membrane, similar to endogenous stx11 (Figure 1C). When J774/mV-stx11 cells were stimulated with LPS, TLR4 surface expression was generally similar to that of the control cells overexpressing mVenus but was significantly up-regulated at 4 h after LPS stimulation compared with the levels in control cells (Figure 6, A and B). The overexpression of mV-stx11 had little effect on TLR4 surface expression at both steady state and after 1 h of LPS stimulation compared with expression in mVenus controls (Figure 6, A and B), suggesting that even overexpressed stx11
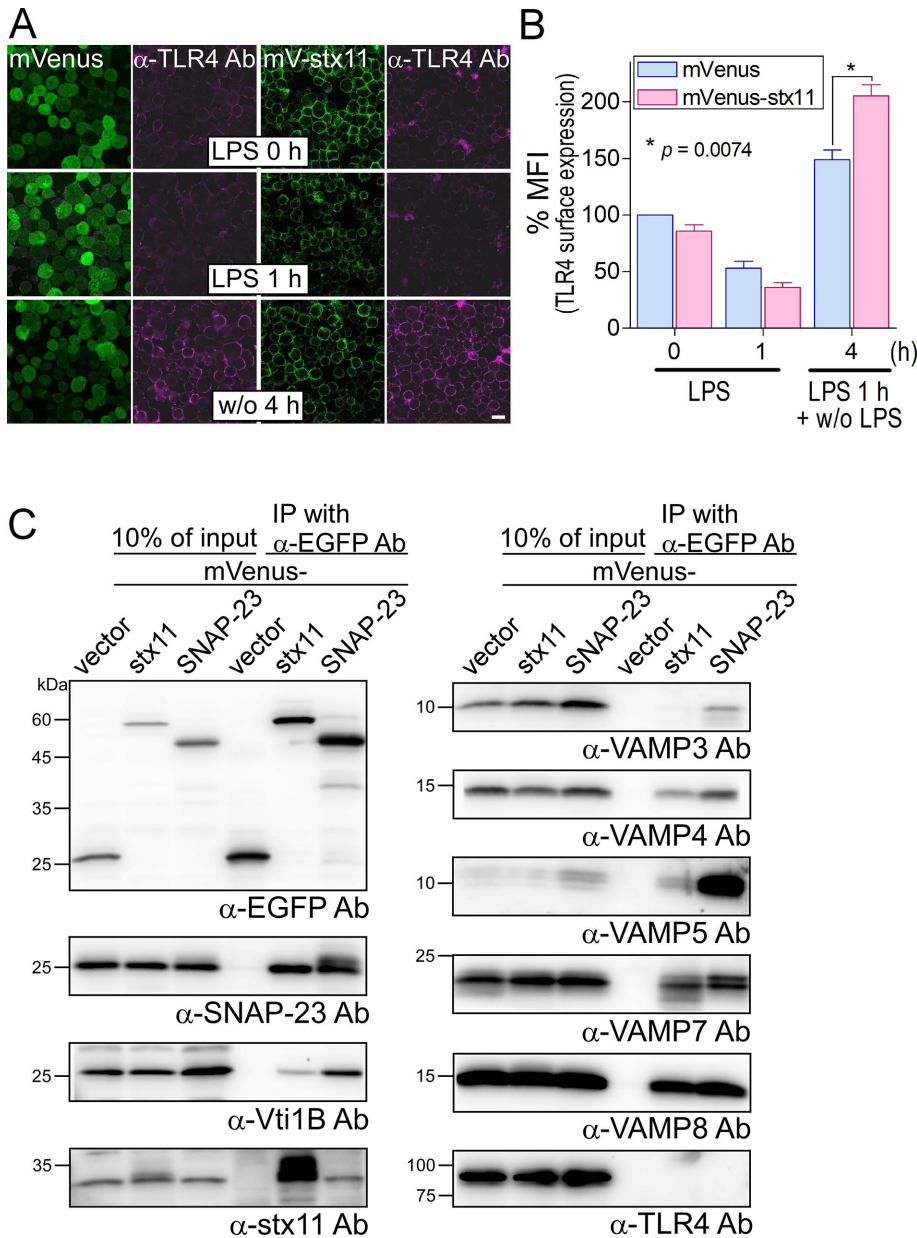
FIGURE 6: Overexpression of mVenus-stx11 enhances the replenishment of TLR4 on the plasma membrane in LPS-stimulated macrophages. (A) J774 cells stably overexpressing mVenus or mVenus-stx11 (mV-stx11) were treated with LPS (1 μg/ml) for 1 h (LPS 1 h). After LPS was washed out, the cells were further incubated without LPS for another 4 h (w/o 4 h). TLR4 surface expression was visualized as described in Figure 2A. Scale bar: 10 μm. (B) Fluorescence intensity of TLR4 surface expression of each cell (of at least 30 cells) from A was quantified using ImageJ. Each intensity value was normalized to that of mVenus cells in the absence of LPS, defined as 100%. Data are presented as the means ± SE of three independent experiments. Statistical analysis was performed using two-tailed, paired Student's *t* tests. (C) Total lysates from each J774 cell overexpressing mVenus-tagged proteins were coimmunoprecipitated (IP) with anti-EGFP antibodies. Immunocomplexes were subjected to SDS–PAGE followed by Western blotting using the indicated antibodies against SNARE proteins and TLR4. mVenus-stx11 or mVenus-SNAP-23 mutually and efficiently interacted with each endogenous protein.

VAMP3, and VAMP8 in platelets and cytotoxic T-lymphocytes (Offenhäuser *et al.*, 2011; Ye *et al.*, 2012; Halimani *et al.*, 2014; Spessott *et al.*, 2017). To identify a SNARE partner(s) for stx11 during LPS stimulation-induced TLR4 transport, we incubated lysates from J774/mVenus or mV-stx11 cells with anti–enhanced green fluorescent protein (anti-EGFP) antibodies and subjected the immunoprecipitates to SDS–PAGE followed by Western blot analysis with antibodies against several SNARE proteins (Figure 6C). Consistent with previous reports, mV-stx11 more efficiently coprecipitated SNAP-23 than other SNARE proteins, except for VAMP3. mVenus-SNAP-23 coprecipitated endogenous stx11 (Sakurai *et al.*, 2012), whereas all examined SNARE proteins were coprecipitated by mVenus-SNAP-23 more efficiently than was mV-stx11. However, the coprecipitation of TLR4 with both mV-stx11 and mV-SNAP-23 was not observed in this condition.

Because SNAP-23 is a candidate SNARE partner for stx11, we examined the effect of *SNAP-23* knockdown by siRNA on LPS-induced TLR4 replenishment. When J774 cells were transfected with SNAP-23 siRNA as described previously (Sakurai *et al.*, 2012), *SNAP-23*–knockdown cells exhibited significantly decreased TLR4 surface expression compared with that of control cells, even during steady state without LPS stimulation (Supplemental Figure S7, A and B). Western blot analysis showed that SNAP-23 expression was reduced, with no effect on the expression of stx11 or TLR4 in *SNAP-23*–knockdown cells (Supplemental Figure S7C). *SNAP-23* knockdown also significantly suppressed the efficiency of TLR4 surface expression compared with that of control cells during 4 h of culture without LPS after stimulation, similar to the effects of *stx11* knockdown (Figure 3, A and B), whereas SNAP-23 surface localization was unaffected by LPS stimulation (Supplemental Figure S8, A and B). These results indicate that SNAP-23 regulates both constitutive and LPS-induced TLR4 transport to the plasma membrane. However, because *SNAP-23* knockdown suppressed the up-regulation of stx11 surface localization upon LPS stimulation (Supplemental Figure S8, C and D), further investigation is necessary to clarify the relationship between stx11 and SNAP-23 during LPS-induced TLR4 transport.

selectively promotes TLR4 transport to the plasma membrane upon LPS stimulation.
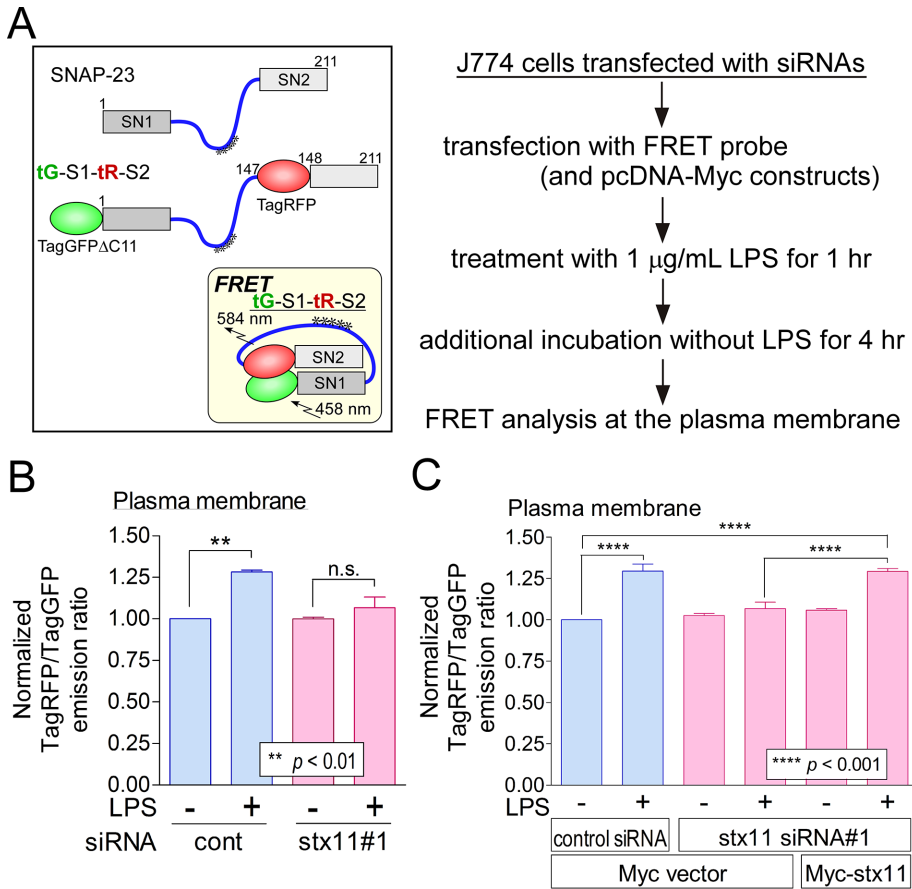
Our results indicate that stx11, a plasma membrane–localized Qa-SNARE, may mediate stimulus-dependent membrane fusion between a vesicle carrying TLR4 and the cell surface. stx11 interacts with several SNARE proteins, such as Vti1b in macrophages and SNAP-23,

stx11 is responsible for the LPS-induced structural alteration of SNAP-23

We previously constructed intramolecular Förster resonance energy transfer (FRET) probes for SNAP-23 to monitor structural alterations during FcR-mediated phagocytosis (Sakurai *et al.*, 2012, 2018). The closed conformation of SNAP-23 (Figure 7A, inset)

FIGURE 7: stx11 is involved in the enhanced FRET signal of the SNAP-23 probe caused by LPS stimulation at the plasma membrane. (A) Schematic of the SNAP-23 FRET probe used in this study. As described previously, truncated TagGFP2 (TagGFPΔC11) and TagRFP were fused to SNAP-23 (Sakurai et al., 2012). The inset shows the predicted conformation of the SNAP-23-based FRET construct (tG-S1-tR-S2) on fusogenic SNARE complex. Asterisks indicate potentially palmitoylated cysteine residues. (B) J774 cells were treated according to the simplified experimental scheme shown to the right of A. FRET measurement at the plasma membrane was performed using live cells expressing tG-S1-tR-S2. The emission peak of TagRFP (at 581 nm) was divided by that of TagGFP2 (at 502 nm; TagRFP/TagGFP) and normalized to the value obtained from cells transfected with control siRNA in the absence of LPS (1 μg/ml), which was arbitrarily set to 1.00. In stx11-knockdown cells, enhanced FRET efficiency was not observed even upon LPS stimulation. Data are presented as the means ± SE of three independent experiments. (C) siRNA-transfected J774 cells were cotransfected with plasmids of tG-S1-tR-S2 and Myc or Myc-stx11. Each FRET efficiency was then measured as described in B. Suppressed FRET efficiency in stx11-knockdown cells was significantly rescued by the expression of Myc-stx11. Data are presented as the means ± SE of three independent experiments. Statistical analyses were performed using one-way ANOVA with Tukey's post hoc tests.

indicating that phosphorylation of SNAP-23 at Ser-95 is not involved in the series of events after LPS stimulation and that SNAP-23 may form a SNARE complex in an LPS-dependent manner. Next, to investigate the correlation between stx11 and the structural alteration of SNAP-23 during LPS-induced TLR4 transport, we transfected J774 cells with control siRNA and stx11 siRNA#1. The enhanced FRET signal in LPS-stimulated control cells was no longer observed in stx11-knockdown cells (Figure 7B). Because stx11 siRNA#1 corresponds to the noncoding region of mouse stx11 mRNA, a Myc-stx11 plasmid was transfected into the stx11-knockdown cells to rescue stx11 function. The FRET signal upon LPS stimulation was recovered to almost the same level as that of control cells by Myc-stx11 expression (Figure 7C), indicating that stx11 is responsible for the structural alteration of SNAP-23 caused by LPS-induced SNARE complex formation on the plasma membrane.

Taken together, these results strongly suggest that stx11 regulates the stimulus-dependent transport of TLR4 to the plasma membrane by cooperating with SNAP-23 in macrophages.

DISCUSSION

TLR4 is one of the most well-studied pattern-recognition receptors and a key regulator of innate immunity and signal transduction. While the stimulation of TLR4 with LPS induces the production of proinflammatory cytokines at the plasma membrane and type I IFN on endosomal compartments, the dysregulation or continuous activation of TLR4 causes severe sepsis, multiorgan failure, and death (Bryant et al., 2010). Therefore, intracellular TLR4 trafficking must be precisely regulated before and after LPS stimulation. However, the molecular mechanisms underlying TLR4 transport toward the plasma membrane upon LPS stimulation remain less understood than TLR4 endocytosis (Liunardy-Jopeace and Gay, 2014). In the

results from proper SNARE complex formation with partner SNARE proteins or its phosphorylation at Ser-95; this structural alteration places inserted TagGFP2 and TagRFP in closer proximity, leading to intramolecular FRET (Sakurai et al., 2012, 2018). Thus, these probes can be used for the detection of SNARE complex formation or for monitoring SNAP-23 phosphorylation at Ser-95. For examination of the effect of LPS stimulation on SNAP-23 dynamics at the plasma membrane, J774 cells were transiently transfected with the plasmid for wild-type (WT) SNAP-23 tG-S1-tR-S2 and its nonphosphorylatable S95A (serine replaced by alanine) mutant probes (Supplemental Figure S9A). The cells were treated with LPS for 1 h and then incubated without LPS for 4 h before FRET analysis. As shown in Supplemental Figure S9B, LPS stimulation caused a significant increase in the FRET signal from the WT and S95A probes,

present study, we found that depletion of stx11, a plasma membrane–localized SNARE protein, in macrophages selectively suppresses TLR4 transport to the plasma membrane, which was induced by IFN-γ or LPS stimulation; this replenished TLR4 on the plasma membrane originated from at least both endocytosis and de novo synthesis in macrophages. Upon LPS stimulation in stx11-knockdown cells, intracellular TLR4 accumulated in the Rab11-positive ERC in the presence of BafA1. Thus, intracellular TLR4, which is not transported to the plasma membrane in stx11-knockdown cells, may be transported from the ERC to lysosomes for degradation. We also showed that SNAP-23 knockdown suppresses TLR4 transport upon LPS stimulation, similar to the results of stx11 knockdown. Finally, our FRET analyses demonstrated that stx11 is actively involved in the LPS-induced structural alteration of SNAP-23 at the
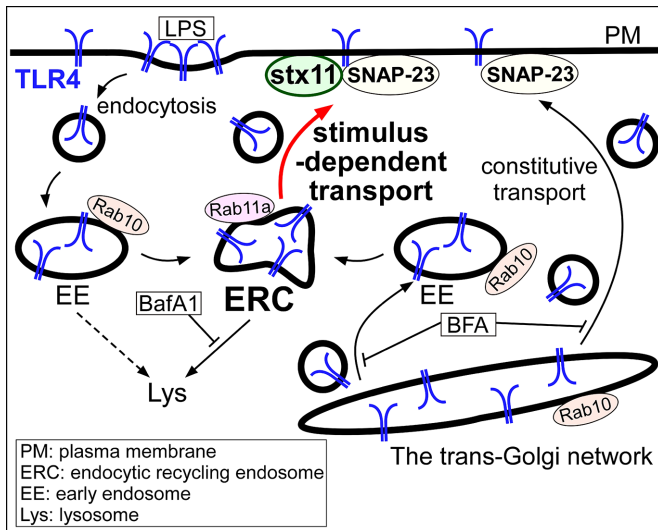
FIGURE 8: Schematic representation of stimulus-dependent transport of TLR4 mediated by stx11 cooperating with SNAP-23 in macrophages. In resting macrophages, some populations of TLR4 are maintained by constitutive transport. When macrophages are stimulated with LPS, TLR4 bound to LPS is endocytosed. Upon LPS stimulation, Rab10 is involved in transport of TLR4 from the Golgi and the early endosome in which it is localized (Wang *et al.*, 2010). Replenished TLR4 upon LPS stimulation contains at least both endocytosed and de novo synthesized populations; the latter shows inhibited transport from the *trans*-Golgi network by BFA. Depletion of stx11 causes mislocalization of TLR4 to lysosomes upon LPS stimulation and TLR4 accumulation in the Rab11a-positive ERC in the presence of BafA1. Thus, stx11 regulates the stimulus-dependent transport of TLR4 to the plasma membrane by cooperating with SNAP-23, which also mediates constitutive transport (see *Discussion*).

plasma membrane. These findings provide the first line of evidence that stx11 regulates stimulus-dependent TLR4 transport to the plasma membrane by cooperating with SNAP-23 in macrophages (Figure 8).

During anterograde transport, folded TLR4 in the ER interacts with TMED7 (cargo receptor) via its cytoplasmic region to exit from the ER to the Golgi apparatus (Liaunardy-Jopeace *et al.*, 2014). Then, TLR4 is transported from the Golgi in both constitutive and LPS-induced pathways via Rab10, which colocalizes with TLR4 in both the Golgi and early endosomes in macrophages (Wang *et al.*, 2010). Because TLR4-mVenus exhibited extensive subcellular localization but was not detected in the Golgi or endocytic compartments, the intracellular pool of TLR4 (potentially in the ER) is unclear. In human monocytes, TLR4 is observed in the ERC and is recruited to phagosomes, including *E. coli*, by Rab11a to promote type I IFN expression (Husebye *et al.*, 2010). In J774 cells, we did not observe TLR4 in the ERC, and stx11 was not involved in TLR4 transport in the constitutive pathway from the Golgi. Therefore, LPS-induced TLR4 transport in macrophages may occur in the stimulus-dependent pathway via the ERC from the Golgi (and ER) or early endosomes, but not in the constitutive pathway (Figure 8). The disruption of LPS-induced TLR4 transport (potentially by the inhibition of membrane fusion between ERC-related vesicles and the plasma membrane) in *stx11*-knockdown cells may cause a switch in the transport direction from the plasma membrane to lysosomes. Because TLR4 transport between the ERC and lysosomes is likely sensitive to BafA1 (Baravalle *et al.*, 2005; Okiyoneda *et al.*, 2006), TLR4 may have accumulated in the Rab11-positive ERC.

Consistent with results in human monocytes/macrophages and human CTLs (Zhang *et al.*, 2008; Dieckmann *et al.*, 2015), we found that stx11 in J774 macrophages is mostly localized on the plasma membrane, while in other types of macrophages, NK cells, and CTLs, stx11 is localized in intracellular structures such as late endosomes/lysosomes and cytolytic granules (Offenhäuser *et al.*, 2011; Dabrazhynetskaya *et al.*, 2012; Halimani *et al.*, 2014; Spessott *et al.*, 2015). Although this discrepancy has not been clearly explained, stx11 essentially functions as a SNARE protein during membrane fusion between intracellular compartments and the plasma membrane (Arneson *et al.*, 2007; Bryceson *et al.*, 2007; Ye *et al.*, 2012). During platelet secretion, stx11 forms SNARE complexes with both VAMP8 and SNAP-23, while stx11 in CTLs does not interact with VAMP8, a recycling endosome-localized R-SNARE (Ye *et al.*, 2012; Halimani *et al.*, 2014; Marshall *et al.*, 2015). In this case, after stx11 delivery from the ERC to the plasma membrane by VAMP8-mediated exocytosis, stx11 forms an acceptor SNARE complex with SNAP-23 to promote membrane fusion of cytolytic granules with the plasma membrane (Marshall *et al.*, 2015). Our data suggested that TLR4 transport in macrophages is mediated by a SNARE complex composed of at least stx11 and SNAP-23. Although stx11 can interact with endosomal VAMPs, such as VAMP4, VAMP7, and VAMP8, the R-SNARE included in this complex is unknown. Delivery of the major histocompatibility complex I components from the ERC to phagosomes requires SNAP-23 and VAMP3 and/or VAMP8 in dendritic cells stimulated by LPS-conjugated microbeads (Nair-Gupta *et al.*, 2014). Thus, while these findings indicate the possibility that VAMP8 is involved in TLR4 transport from the ERC to the plasma membrane in LPS-stimulated macrophages, further studies are needed to identify the functional R-SNARE involved in this process.

IFN-γ is a cytokine produced by T-helper 1 lymphocytes and regulates the antimicrobial activity of macrophages by modulating functions such as phagocytosis and antigen presentation. IFN-γ enhances cell surface expression as well as mRNA expression levels of TLR4 in human monocytes and macrophages (Bosisio *et al.*, 2002), but we did not observe an apparent increase in protein expression in IFN-γ–activated J774 cells. However, we found that the efficiency of FcR- and TLR4-mediated phagocytosis was enhanced. In *stx11*-knockdown cells, normal augmentation of both the uptake of IgG-opsonized zymosan and the expression of LRG47 by IFN-γ activation indicates that the transport of FcR(s) and IFN-γ receptors onto the cell surface is not affected. These receptors may be transported via the constitutive secretory pathway or through intracellular compartment(s) other than the ERC. Although this study focused on the surface expression of TLR4 with respect to the *E. coli* uptake efficiency, other cooperative factors, such as the CD36 scavenger receptor, may also be suppressed in *stx11*-knockdown cells (Cao *et al.*, 2016). In resting J774 cells, *stx11* knockdown does not affect surface expression of TLR4. Therefore, in both control and stx11 siRNA#1–transfected cells, the effect of LPS stimulation for at least 1 h appears similar; indeed, the endocytotic profile of both cells is comparable. These results indicated that formation of the SNARE complex including stx11 is one of the targets of IFN-γ or LPS during TLR4 transport. This is strongly supported by analysis of SNAP-23 intramolecular FRET probes. During FcR-mediated phagocytosis, uptake efficiency is regulated by SNAP-23 phosphorylation at Ser-95 (Sakurai *et al.*, 2018), whereas this phosphorylation is not involved in the structural alteration of SNAP-23 induced by LPS stimulation. In future studies, we aim to explore the regulatory mechanism by which formation of the stx11/SNAP-23 complex is activated in macrophages and to clarify

the effects of SNARE functions on the activation of TLR4 signaling pathways.

MATERIALS AND METHODS

Antibodies

Polyclonal antibodies against EGFP, syntaxin 11, VAMP3, VAMP5, and VAMP7 were prepared as described previously (Sakurai et al., 2012). The remaining antibodies were obtained from the following commercial sources; TLR4 (25), LAMP-1 (1D4B), and LRG47 (A-19) from Santa Cruz Biotechnology (Santa Cruz, CA); Vti1B, VAMP4, SNAP-23, FLAG, and β-actin from Sigma-Aldrich (St. Louis, MO); VAMP8 from Synaptic Systems (Göttingen, Germany); Rab11, GM130, and EEA1 from BD Transduction Laboratories (San Jose, CA); and glyceraldehyde-3-phosphate dehydrogenase from Ambion (Austin, TX).

Cell culture

J774 cells were obtained from the Riken Cell Bank (Tsukuba, Japan) and cultured in RPMI 1640 medium (Fujifilm Wako Pure Chemical Industries, Osaka, Japan) supplemented with 10% fetal bovine serum (FBS) at 37°C in 5% CO_2. J774 cells stably expressing mVenus (mV) and mVenus-syntaxin 11 (mV-stx11) were maintained in RPMI supplemented with 10% FBS and 2 μM puromycin. J774 cells stably expressing TLR4 (I254V)-mVenus and MD2-Flag (TLR4-mV and MD2-Flag) were maintained in RPMI with 10% FBS in the presence of 2 μM puromycin and 0.7 μM blasticidin.

Treatment with IFN-γ and LPS

J774 cells were treated with recombinant murine IFN-γ (at a final concentration of 10–200 U/ml; PeproTec, Rocky Hill, NJ) for 18 h and then used for subsequent experiments. J774 cells and J774/TLR4-mV + MD2-Flag cells were treated with LPS from E. coli O26:B6 (at a final concentration of 1 μg/ml; Sigma-Aldrich) for 1 h. After treatment for 1 h, the LPS-containing medium was completely removed, and the cells were incubated in culture medium without LPS for 2 or 4 h. The cells were used for subsequent experiments.

siRNA experiments

An siRNA duplex with 52% GC content (5′-GUACCGCACGUCAU-UCGUAUC-3′; Sigma-Aldrich) was used as a control. RNA duplexes used for targeting were stx11 siRNA#1 (5′-GAAUAGUUGUUAAU-AUCCATT-3′) and siRNA#2 (5′-GACAUGUCGGGCGAGCAGATT-3′) corresponding to the noncoding region and the open reading frame of mouse stx11 mRNA, respectively. The RNA duplex for mouse SNAP-23 was previously described (Sakurai et al., 2012). J774 cells or J774/TLR4-mV + MD2-Flag cells were transfected with control (20–100 nM final concentration), stx11 siRNAs (20–100 nM final concentration), or SNAP-23 siRNAs (100 nM final concentration) using HiPerFect transfection reagent (Qiagen, Valencia, CA) according to the manufacturer's instructions. At 3 d after transfection, the cells were used for subsequent experiments.

Expression vectors and the establishment of stable transfectants

stx11, TLR4, and MD2 cDNAs were obtained by reverse transcription PCR using total RNA extracted from J774 cells. The cDNAs were cloned into the pmVenus-C1, pmVenus-N1, pcDNA-Myc-C1, or pFLAG vectors. TLR4 of J774 cells (derived from BALB/c mice) contains a V254I mutation, resulting in the replacement of Val-254 by Ile, compared with that derived from C57BL/6 mice (Tsukamoto et al., 2013). Because this mutation results in reduced TLR4 surface

expression (Tsukamoto et al., 2013), pTLR4 (I254V)-mVenus was created by overlap PCR and confirmed by DNA sequencing. C57BL/6-type TLR4 (I254V) is termed "TLR4" in this study.

J774 cell lines stably expressing mVenus, mVenus-tagged proteins (mV-stx11or TLR4-mV), or FLAG-tagged MD2 proteins were established by infection with recombinant retroviruses generated using cDNAs of mVenus or mVenus-tagged proteins cloned into the pCXpur vector and the cDNA of MD2-Flag protein cloned into the pCXblast vector, respectively (Akagi et al., 2003).

Analysis of phagocytosis with opsonized Texas Red–conjugated zymosan or E. coli-mCherry-mVenus particles

The opsonized Texas Red–conjugated zymosan assay was performed as described previously (Hatsuzawa et al., 2009; Sakurai et al., 2012). The E. coli-mCherry-mVenus phagocytotic assay was also performed as described previously (Morita et al., 2017). For analysis of the association efficiency, cells were incubated for 30 min on ice with E. coli-mCherry-mVenus particles and then washed with ice-cold phosphate-buffered saline (PBS). Washed cells were fixed with 4% paraformaldehyde (PFA)/PBS, and then the fluorescence of particles associated with the cells was measured using an Infinite F500 microplate reader (Tecan, Kawasaki, Japan) at an excitation wavelength of 535 nm and an emission wavelength of 612 nm.

Western blotting and immunoprecipitation

Cell lysates with extraction buffer (20 mM HEPES-KOH, pH 7.2, 100 mM KCl, 2 mM EDTA, 1% Triton X-100, 1 mM dithiothreitol, and a protease inhibitor cocktail [Nacalai Tesque, Kyoto, Japan]) were treated at 95°C with 5X SDS–PAGE sample buffer. The samples were analyzed by Western blotting using various antibodies. Immunoreactive proteins were visualized using ImmunoStar Zeta (Fujifilm Wako Pure Chemical Industries) and the ImageQuant LAS-4000 system (GE Healthcare Bio-Sciences, Tokyo, Japan) (Morita et al., 2017). For immunoprecipitation, lysates from J774 cells stably expressing mVenus-tagged proteins were incubated with anti-EGFP antibodies for 30 min at 4°C. Protein A-Sepharose (GE Healthcare) was then added, and the mixture was incubated for 16 h at 4°C with gentle rotation. Subsequently, beads were washed with extraction buffer, and the immune complexes were eluted with SDS–PAGE sample buffer. After SDS–PAGE, the samples were analyzed by Western blotting as described earlier.

Immunostaining

J774 cells were fixed with 100% methanol for 7 min at –20°C and incubated with Blocking One solution (Nacalai Tesque) for 30 min at 25°C. Subsequently, the cells were treated with anti-stx11 antibodies and stained with anti-rabbit IgG antibodies conjugated to Alexa 488 (Thermo Fisher Scientific, Waltham, MA). For J774/TLR4-mV and MD2-Flag cells, the cells were fixed with 10% trichloroacetic acid for 10 min on ice and permeabilized with 0.2% Triton X-100/PBS for 5 min at 25°C. After blocking with 2% bovine serum albumin (BSA)/PBS, the cells were treated with primary antibodies (except anti-Rab11 antibodies) followed by staining with secondary antibodies (Alexa 488 and/or Alexa 568). For double staining of Rab11 and marker proteins, cells were immunostained with anti-Rab11 antibodies as described earlier and then fixed again with 4% PFA/PBS for 20 min at 25°C. After blocking with 2% BSA/PBS, the cells were treated with anti-EGFP antibodies followed by staining with anti-rabbit secondary antibodies (Alexa 488). For detection of TLR4 cell surface expression, the cells incubated with Blocking One solution on ice for 30 min were treated with anti-TLR4 antibodies for 1 h on

ice followed by staining with anti-mouse secondary antibodies (Alexa 488). The cells were then fixed with 4% PFA/PBS for 30 min on ice. Images were obtained using an LSM710 confocal laser-scanning microscope with a Plan-Apochromat 63×/1.40 oil DIC M27 objective lens (Carl-Zeiss, Oberkochen, Germany). Quantification of TLR4 cell surface expression was performed using ImageJ v. 1.52a (National Institutes of Health, Bethesda, MD).

FRET probes
The FRET probe for SNAP-23 consisted of TagGFPΔC11 (1–227), which lacked 11 C-terminal residues from the pTagGFP2 vector, and TagRFP-t (1–237), in which Ser-162 of the pTagRFP-N vector was replaced with Thr, as described previously (Sakurai *et al.*, 2012). Methods for the construction of the tG-S1-tR-S2 (TagGFPΔC11 [1–227]-SNAP-23 [1–147]-TagRFP-t [1–237]-SNAP-23 [148–211]) and tG-S1-tR-S2 S95A probes (serine at 95th position replaced by alanine) were described previously (Sakurai *et al.*, 2012, 2018).

FRET analysis
At 48 h after transfection with siRNAs, FRET probes for SNAP-23 were expressed in J774 cells together with the Myc vector or Myc-tagged syntaxin11 using XtremeGENE HP DNA Transfection Reagent (Roche Diagnostics K.K., Tokyo, Japan) according to the manufacturer's instructions. At 20 h after FRET probe transfection, the cells were incubated in the presence or absence of 1 µg/ml LPS for 1 h. The LPS-containing medium was completely removed, and the cells were incubated in the culture medium without LPS for 4 h before analysis. Fluorescence spectra of the probes on the plasma membranes of live cells were obtained using the LSM780meta laser-scanning microscope (Carl Zeiss) at an excitation wavelength of 458 nm. Before measurements were taken, the dynamic range at each wavelength was calibrated using a standard solution according to the manufacturer's instructions. Analysis of the spectrum with a fluorescence intensity of ~250 arbitrary units at 503 nm was performed using the LSM780meta microscope. FRET efficiency is represented as the 582/503-nm emission ratio.

Statistical analysis
Data are presented as mean ± SE. Differences between the groups were analyzed by two-tailed, paired Student's *t* tests or by one-way analysis of variance (ANOVA) with Tukey's post hoc test using GraphPad Prism (GraphPad Software, San Diego, CA). Statistical significance was defined as $p < 0.05$.

REFERENCES
Akagi T, Sasai K, Hanafusa H (2003). Refractory nature of normal human diploid fibroblasts with respect to oncogene-mediated transformation. Proc Natl Acad Sci USA 100, 13567–13572.

Akira S, Takeda K (2004). Toll-like receptor signalling. Nat Rev Immunol 4, 499–511.

Arneson LN, Brickshawana A, Segovis CM, Schoon RA, Dick CJ, Leibson PJ (2007). Cutting edge: syntaxin 11 regulates lymphocyte-mediated secretion and cytotoxicity. J Immunol 179, 3397–3401.

Baravalle G, Schober D, Huber M, Bayer N, Murphy RF, Fuchs R (2005). Transferrin recycling and dextran transport to lysosomes is differentially affected by bafilomycin, nocodazole, and low temperature. Cell Tissue Res 320, 99–113.

Bosisio D, Polentarutti N, Sironi M, Bernasconi S, Miyake K, Webb GR, Martin MU, Mantovani A, Muzio M (2002). Stimulation of Toll-like receptor 4 expression in human mononuclear phagocytes by interferon-gamma: a molecular basis for priming and synergism with bacterial lipopolysaccharide. Blood 99, 3427–3431.

Bryant CE, Spring DR, Gangloff M, Gay NJ (2010). The molecular basis of the host response to lipopolysaccharide. Nat Rev Microbiol 8, 8–14.

Bryceson YT, Rudd E, Zheng C, Edner J, Ma D, Wood SM, Bechensteen AG, Boelens JJ, Celkan T, Farah RA, *et al.* (2007). Defective cytotoxic lymphocyte degranulation in syntaxin-11 deficient familial hemophagocytic lymphohistiocytosis 4 (FHL4) patients. Blood 110, 1906–1915.

Cao D, Luo J, Chen D, Xu H, Shi H, Jing X, Zang W (2016). CD36 regulates lipopolysaccharide-induced signaling pathways and mediates the internalization of *Escherichia coli* in cooperation with TLR4 in goat mammary gland epithelial cells. Sci Rep 6, 23132.

Chang HF, Bzeih H, Chitirala P, Ravichandran K, Sleiman M, Krause E, Hahn U, Pattu V, Rettig J (2017). Preparing the lethal hit: interplay between exo- and endocytic pathways in cytotoxic T lymphocytes. Cell Mol Life Sci 74, 399–408.

Collins LE, DeCourcey J, Rochfort KD, Kristek M, Loscher CE (2015). A role for syntaxin 3 in the secretion of IL-6 from dendritic cells following activation of Toll-like receptors. Front Immunol 5, 691.

Dabrazhynetskaya A, Ma J, Guerreiro-Cacais AO, Arany Z, Rudd E, Henter JI, Karre K, Levitskaya J, Levitsky V (2012). Syntaxin 11 marks a distinct intracellular compartment recruited to the immunological synapse of NK cells to colocalize with cytotoxic granules. J Cell Mol Med 16, 129–141.

de Saint Basile G, Menasche G, Fischer A (2010). Molecular mechanisms of biogenesis and exocytosis of cytotoxic granules. Nat Rev Immunol 10, 568–579.

Dieckmann NM, Hackmann Y, Arico M, Griffiths GM (2015). Munc18-2 is required for syntaxin 11 Localization on the plasma membrane in cytotoxic T-lymphocytes. Traffic 16, 1330–1341.

D'Orlando O, Zhao F, Kasper B, Orinska Z, Muller J, Hermans-Borgmeyer I, Griffiths GM, Zur Stadt U, Bulfone-Paus S (2013). Syntaxin 11 is required for NK and CD8⁺ T-cell cytotoxicity and neutrophil degranulation. Eur J Immunol 43, 194–208.

Fasshauer D, Sutton RB, Brunger AT, Jahn R (1998). Conserved structural features of the synaptic fusion complex: SNARE proteins reclassified as Q- and R-SNAREs. Proc Natl Acad Sci USA 95, 15781–15786.

Halimani M, Pattu V, Marshall MR, Chang HF, Matti U, Jung M, Becherer U, Krause E, Hoth M, Schwarz EC, Rettig J (2014). Syntaxin11 serves as a t-SNARE for the fusion of lytic granules in human cytotoxic T lymphocytes. Eur J Immunol 44, 573–584.

Hatsuzawa K, Hashimoto H, Hashimoto H, Arai S, Tamura T, Higa-Nishiyama A, Wada I (2009). Sec22b is a negative regulator of phagocytosis in macrophages. Mol Biol Cell 20, 4435–4443.

Hellewell AL, Foresti O, Gover N, Porter MY, Hewitt EW (2014). Analysis of familial hemophagocytic lymphohistiocytosis type 4 (FHL-4) mutant proteins reveals that S-acylation is required for the function of syntaxin 11 in natural killer cells. PLoS One 9, e98900.

Hong W, Lev S (2014). Tethering the assembly of SNARE complexes. Trends Cell Biol 24, 35–43.

Husebye H, Aune MH, Stenvik J, Samstad E, Skjeldal F, Halaas O, Nilsen NJ, Stenmark H, Latz E, Lien E, *et al.* (2010). The Rab11a GTPase controls Toll-like receptor 4-induced activation of interferon regulatory factor-3 on phagosomes. Immunity 33, 583–596.

Jahn R, Scheller RH (2006). SNAREs—engines for membrane fusion. Nat Rev Mol Cell Biol 7, 631–643.

Kagan JC, Su T, Horng T, Chow A, Akira S, Medzhitov R (2008). TRAM couples endocytosis of Toll-like receptor 4 to the induction of interferon-beta. Nat Immunol 9, 361–368.

Liaunardy-Jopeace A, Bryant CE, Gay NJ (2014). The COP II adaptor protein TMED7 is required to initiate and mediate the delivery of TLR4 to the plasma membrane. Sci Signal 7, ra70.

Liaunardy-Jopeace A, Gay NJ (2014). Molecular and cellular regulation of Toll-like receptor-4 activity induced by lipopolysaccharide ligands. Front Immunol 5, 473.

MacMicking JD (2004). IFN-inducible GTPases and immunity to intracellular pathogens. Trends Immunol 25, 601–609.

Marshall MR, Pattu V, Halimani M, Maier-Peuschel M, Muller ML, Becherer U, Hong W, Hoth M, Tschernig T, Bryceson YT, Rettig J (2015). VAMP8-dependent fusion of recycling endosomes with the plasma membrane facilitates T lymphocyte cytotoxicity. J Cell Biol 210, 135–151.

Morita M, Sawaki K, Kinoshita D, Sakurai C, Hori N, Hatsuzawa K (2017). Quantitative analysis of phagosome formation and maturation using an *Escherichia coli* probe expressing a tandem fluorescent protein. J Biochem 162, 309–316.

Naegelen I, Plancon S, Nicot N, Kaoma T, Muller A, Vallar L, Tschirhart EJ, Brechard S (2015). An essential role of syntaxin 3 protein for granule exocytosis and secretion of IL-1alpha, IL-1beta, IL-12b, and CCL4 from differentiated HL-60 cells. J Leukoc Biol 97, 557–571.

Nair-Gupta P, Baccarini A, Tung N, Seyffer F, Florey O, Huang Y, Banerjee M, Overholtzer M, Roche P, Tampe R, *et al*. (2014). TLR signals induce phagosomal MHC-I delivery from the endosomal recycling compartment to allow cross-presentation. Cell 158, 506–521.

Offenhäuser C, Lei N, Roy S, Collins BM, Stow JL, Murray RZ (2011). Syntaxin 11 binds Vti1b and regulates late endosome to lysosome fusion in macrophages. Traffic 12, 762–773.

Okiyoneda T, Niibori A, Harada K, Kohno T, Hashimoto Y, Kusuhara H, Takada T, Shuto T, Suico MA, Sugiyama Y, Kai H (2006). Bafilomycin A1-sensitive pathway is required for the maturation of cystic fibrosis transmembrane conductance regulator. Biochim Biophys Acta 1763, 1017–1023.

Prekeris R, Klumperman J, Scheller RH (2000). Syntaxin 11 is an atypical SNARE abundant in the immune system. Eur J Cell Biol 79, 771–780.

Randow F, Seed B (2001). Endoplasmic reticulum chaperone gp96 is required for innate immunity but not cell viability. Nat Cell Biol 3, 891–896.

Sakurai C, Hashimoto H, Nakanishi H, Arai S, Wada Y, Sun-Wada GH, Wada I, Hatsuzawa K (2012). SNAP-23 regulates phagosome formation and maturation in macrophages. Mol Biol Cell 23, 4849–4863.

Sakurai C, Itakura M, Kinoshita D, Arai S, Hashimoto H, Wada I, Hatsuzawa K (2018). Phosphorylation of SNAP-23 at Ser95 causes a structural alteration and negatively regulates Fc receptor-mediated phagosome formation and maturation in macrophages. Mol Biol Cell 29, 1753–1762.

Spessott WA, Sanmillan ML, McCormick ME, Kulkarni VV, Giraudo CG (2017). SM protein Munc18-2 facilitates transition of syntaxin 11-mediated lipid mixing to complete fusion for T-lymphocyte cytotoxicity. Proc Natl Acad Sci USA 114, E2176–E2185.

Spessott WA, Sanmillan ML, McCormick ME, Patel N, Villanueva J, Zhang K, Nichols KE, Giraudo CG (2015). Hemophagocytic lymphohistiocytosis caused by dominant-negative mutations in STXBP2 that inhibit SNARE-mediated membrane fusion. Blood 125, 1566–1577.

Takahashi K, Shibata T, Akashi-Takamura S, Kiyokawa T, Wakabayashi Y, Tanimura N, Kobayashi T, Matsumoto F, Fukui R, Kouro T, *et al*. (2007). A protein associated with Toll-like receptor (TLR) 4 (PRAT4A) is required for TLR-dependent immune responses. J Exp Med 204, 2963–2976.

Takeuchi O, Akira S (2010). Pattern recognition receptors and inflammation. Cell 140, 805–820.

Tsukamoto H, Fukudome K, Takao S, Tsuneyoshi N, Ohta S, Nagai Y, Ihara H, Miyake K, Ikeda Y, Kimoto M (2013). Reduced surface expression of TLR4 by a V254I point mutation accounts for the low lipopolysaccharide responder phenotype of BALB/c B cells. J Immunol 190, 195–204.

Wakabayashi Y, Kobayashi M, Akashi-Takamura S, Tanimura N, Konno K, Takahashi K, Ishii T, Mizutani T, Iba H, Kouro T, *et al*. (2006). A protein associated with Toll-like receptor 4 (PRAT4A) regulates cell surface expression of TLR4. J Immunol 177, 1772–1779.

Wang D, Lou J, Ouyang C, Chen W, Liu Y, Liu X, Cao X, Wang J, Lu L (2010). Ras-related protein Rab10 facilitates TLR4 signaling by promoting replenishment of TLR4 onto the plasma membrane. Proc Natl Acad Sci USA 107, 13806–13811.

Ye S, Karim ZA, Al Hawas R, Pessin JE, Filipovich AH, Whiteheart SW (2012). Syntaxin-11, but not syntaxin-2 or syntaxin-4, is required for platelet secretion. Blood 120, 2484–2492.

Zanoni I, Ostuni R, Marek LR, Barresi S, Barbalat R, Barton GM, Granucci F, Kagan JC (2011). CD14 controls the LPS-induced endocytosis of Toll-like receptor 4. Cell 147, 868–880.

Zhang S, Ma D, Wang X, Celkan T, Nordenskjold M, Henter JI, Fadeel B, Zheng C (2008). Syntaxin-11 is expressed in primary human monocytes/macrophages and acts as a negative regulator of macrophage engulfment of apoptotic cells and IgG-opsonized target cells. Br J Haematol 142, 469–479.

Zhou P, Bacaj T, Yang X, Pang ZP, Sudhof TC (2013). Lipid-anchored SNAREs lacking transmembrane regions fully support membrane fusion during neurotransmitter release. Neuron 80, 470–483.